Localized eigenmodes of the overlap operator and their impact on the eigenvalue distribution

Anna Hasenfratz* and Roland Hoffmann†
Department of Physics, University of Colorado, Boulder, CO-80309-390

Stefan Schaefer‡
NIC, DESY, Platanenallee 6, D-15738 Zeuthen, Germany

Abstract

In a system where chiral symmetry is spontaneously broken, the low energy eigenmodes of the continuum Dirac operator are extended. On the lattice, due to discretization effects, the Dirac operator can have localized eigenmodes that affect physical quantities sensitive to chiral symmetry. While the infrared eigenmodes of the Wilson Dirac operator are usually extended even on coarse lattices, the chiral overlap operator has many localized eigenmodes in the physical region, especially in mixed action simulations. Depending on their density, these modes can introduce strong lattice artifacts. The effect can be controlled by changing the parameters of the overlap operator, in particular the clover improvement term and the center of the overlap projection.

*Electronic address: anna@eotvos.colorado.edu
†Electronic address: hoffmann@pizero.colorado.edu
‡Electronic address: stefan.schaefer@desy.de

I. INTRODUCTION

Mixed action simulations with overlap valence quarks on dynamical configurations generated with a non-chiral fermion action can combine the advantages of chiral operators in the measurement with relatively fast configuration generation. The success of this approach depends to a large extent on how well the valence action matches the sea action. At the very least the valence action should not introduce any new large lattice artifacts. In this paper we draw attention to a non-perturbative lattice artifact, due to localized eigenmodes of the Dirac operator, that strongly affects the overlap operator, especially in mixed action simulations.

In the phase where chiral symmetry is spontaneously broken, the low energy eigenmodes of the continuum Dirac operator are expected to be extended, delocalized. We have investigated the localization properties of the eigenmodes of the Wilson Dirac operator and several different overlap operators. We found that while both the Wilson and overlap operators have localized eigenmodes, in case of the Wilson Dirac operator these modes usually do not mix with the infrared modes but they can become part of the low energy spectrum of the overlap operator. The source of these modes are dislocations and the localized modes of the overlap operator can be related to the localized modes of the kernel operator. The density of these non-physical overlap modes depend on the kernel operator, on the parameters of the overlap construction, on the gauge configurations (quenched or dynamical or mixed action) and on the lattice spacing and can be particularly large in case of quenched or mixed action simulations.

The physical effect of the localized eigenmodes is easily observable when the distribution of the Dirac eigenvalue spectrum is compared to the predictions of Random Matrix Theory (RMT). RMT relies on very basic assumptions and in quenched systems the only condition for its validity is that the wave functions of the non-zero Dirac eigenmodes are extended over the whole volume [1, 2]. We show that the deviations between RMT predictions and the measured distributions are closely related to the density of the localized overlap eigenmodes. We argue that some of the same lattice artifacts are responsible for the rather large scaling violation effects observed in the topological susceptibility as well. Our observations suggests that in order to minimize scaling violations in valence overlap simulations it is not sufficient to rely on automatic perturbative $O(a)$ improvement but that non-perturbative lattice artifacts due to dislocations also have to be considered.

II. NOTATIONS AND PARAMETERS

We want to study the lattice artifacts due to the localized low energy eigenmodes of the overlap operator. We consider several different overlap operators, and in order to facilitate the comparison between them we calculate their eigenvalues on the same quenched configuration set, consisting of about 1000 12^4 configurations with Wilson plaquette action at $\beta = 5.8458$ ($a \approx 0.12$fm).

Action	Smearing	$c_{\rm SW}$	$\lambda_{\rm crit}$	R_0	$\Delta R_0 = R_0 - \lambda_{\rm crit}$
S1	n-HYP	0	0.30	1.0	0.70
S2	n-HYP	0	0.30	0.7	0.40
S3	n-HYP	1	0.08	1.0	0.92
S4	n-HYP	1	0.08	0.3	0.22
T1	thin	0	0.90	1.4	0.50

Table I: The parameters of the overlap action considered in this study. $\lambda_{\rm crit}$ is the approximate (real) lower bound of the complex kernel spectrum at $\beta = 5.8458$ as explained in Sect.II.

Our definition of the massless overlap operator is

$$D_{\rm ov} = R_0 \left(1 + d(d^\dagger d)^{-1/2}\right) \ , \quad d = D_K - R_0 \ , \tag{1}$$

where D_K is the kernel operator and R_0 denotes the center of the overlap projection. We chose D_K to be the Wilson operator with n-HYP smeared gauge connections [3, 4], both unimproved and with tree level ($c_{\rm SW} = 1$) clover improvement. These kernel operators were motivated by our ongoing dynamical simulations [4].

The choice of the parameter R_0 in the overlap construction is rather arbitrary, as long as it is larger than the eigenvalues of the physical, infrared modes of the kernel operator but smaller than the doubler modes, and the resulting overlap operator is local. Since the additive mass renormalization and hence the location of the IR edge of the spectrum varies with the kernel action, the quantity $\Delta R_0 = R_0 - \lambda_{\rm crit}$, with $\lambda_{\rm crit}$ the location where the IR edge of the complex spectrum intersects the real axis, characterizes the overlap operator better than R_0 itself. We have chosen two different ΔR_0 values with both of our kernel actions. The parameters are listed in Table I, where for reference we also give the parameters of the overlap action used in [5] on configurations similar to ours.

The parameter $R_0 = 1.4$ in [5] was chosen by maximizing the locality of the thin link unimproved overlap action $T1$. The localization of our overlap actions varies depending on their parameters, but all of them are local.

III. THE EIGENVALUE SPECTRUM OF THE KERNEL AND OVERLAP DIRAC OPERATORS

In this section we study the eigenvalue spectrum and the localization properties of the eigenmodes of both the kernel and the overlap operators. Figure 1 shows the 40 lowest magnitude eigenvalues on 100 configurations with both the $c_{\rm SW} = 1$ and $c_{\rm SW} = 0$ kernel actions. (The apparent half-moon shape on the right is only an artifact, due to identifying only the lowest magnitude eigenvalues.) From Figure 1 we approximate $\lambda_{\rm crit} = 0.08$ and 0.30 for the $c_{\rm SW} = 1$ and $c_{\rm SW} = 0$ actions, as listed in Table I. Note that the spectrum of the n-HYP smeared $c_{\rm SW} = 1$ operator appears much more chiral than the unimproved one, its

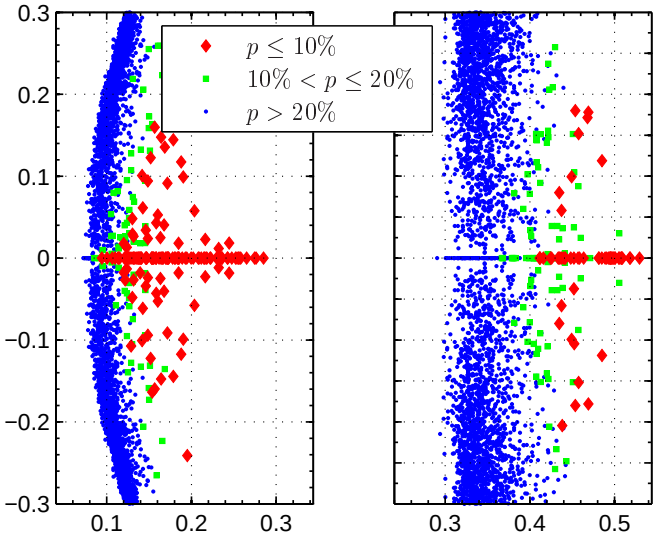

Figure 1: The spectrum of the two kernel operators used in this study. Both are n-HYP smeared Wilson operators, one with tree level $c_{\rm SW} = 1$ clover coefficient (left panel), the other with $c_{\rm SW} = 0$ (right panel). The different plot symbols correspond to different localization levels of the corresponding eigenvectors .

eigenvalues are concentrated around a unit circle. This is what makes this action appealing in dynamical simulations [4].

A simple and very intuitive measure of the localization of the eigenmodes is the participation number or inverse of the inverse participation ratio IPR [6]

$$\begin{aligned} p &= IPR^{-1} \\ IPR &= V \sum_x |\psi(x)|^4 \,, \end{aligned} \tag{2}$$

where $\psi(x)$ is the normalized eigenvector of the Dirac operator. p varies between $1/V$ and 1, the latter corresponding to a uniform wave function, the former to one localized on one lattice site. The participation number is only a qualitative measure: while a very small p certainly implies a localized mode, a large value does not necessarily mean a coherent extended one. In addition, the participation number is sensitive to local fluctuations, so direct comparison is only meaningful between configurations with similar level of vacuum fluctuations (or plaquette values). For reference we mention that for a fully separated smooth instanton–anti-instanton pair of radii $\rho/a = 2$ the participation number is $p \approx 0.06$ on 12^4 lattices. Therefore one expects that participation numbers $p < 0.1$, probably even $p < 0.2$, correspond to a localized mode.

In Figure 1 the different plotting symbols correspond to different participation numbers of the eigenmodes, and one observes a strong correlation between p and $\Delta\lambda$, the radial distance of the eigenvalue from the outer edge of the approximate circle. Toward the center of the eigenvalue circle all modes appear to be localized with small p for both actions. However

the spectrum of the clover improved action has many more localized modes in the vicinity of the physical, IR range. The spectra in Figure 1 are on 12^4 lattices. We have investigated the localization of the modes also on 16^4 volumes, though with smaller statistics. We found that the localization of the kernel operator eigenmodes is not qualitatively different in larger volumes. The number of eigenmodes is proportional to the volume, the participation number decreases with increasing $\Delta\lambda$ and the number of localized modes in a $1/V$ region around the real axis is approximately independent of the volume. There are particularly many localized real modes, especially with $c_{\rm SW} = 1$.

Since the participation number is strongly correlated with $\Delta\lambda$, the distance form the infra-red edge of the spectrum, it is meaningful to define the average participation $\bar{p}(\Delta\lambda)$ as the average of the participation number of eigenvalues in the vicinity of the real axis at $\Delta\lambda$. If the typical eigenmodes at some $\Delta\lambda$ value correspond to extended modes, their average participation $\bar{p}$ should be volume independent, while in the region where most of the eigenmodes are localized, $\bar{p}$ will decrease with the inverse of the volume. Comparing data on 12^4 and 16^4 lattices we see constant $\bar{p}$ values for $\Delta\lambda < 0.03$ and $1/V$ dependence for $\Delta\lambda \geq 0.05$ for the $c_{SW} = 1$ spectrum. This finite volume analysis suggests that on the 12^4 lattices eigenmodes with participation number $p < 0.40$ at $\Delta\lambda \approx 0.05$ are already localized. This in turn indicates that the overlap operator with the small $\Delta R = 0.22$ of action S4 is local since the center of the overlap projection is still beyond the physical, extended eigenmodes.

The overlap construction "projects" all the modes of the kernel operator to the Ginsparg-Wilson circle. Of course it does more than just simply project the modes - opposite chirality modes from the real axis merge and split into complex modes, and in general the wave function, and with it the participation number of the modes, can change.

An example of how the overlap construction transforms the kernel modes is given in Figure 2 where a few of the low energy eigenvalues of the $c_{SW} = 1$ kernel operator and the corresponding overlap operator are shown on a configuration with a localized infrared overlap eigenmode. All but one of the kernel eigenmodes in Figure 2 are extended with large participation numbers. The only exception is the mode in the inner part of the circle that has participation number $p \approx 0.04$. The eigenmodes of the overlap operator are also extended with one exception, the mode with the lowest imaginary value has $p \approx 0.08$.

The extended overlap eigenmodes all connect strongly to a kernel mode, with overlap between the wave functions, i.e. the absolute value of their inner product, of 80% or larger. The grey lines in Figure 2 connect the overlap modes with the kernel mode with which they have the highest overlap. It appears that the extended, near infrared eigenmodes change little under the overlap projection, their eigenvalues basically move out straight to the Ginsparg-Wilson circle. This is likely so because the n-HYP smeared kernel already has excellent chiral properties and we would expect the situation to be quite different with an unsmeared kernel.

The localized modes, on the other hand, behave differently. There is only one localized overlap and one localized kernel mode in Fig. 2. The wave function of both of these modes are sharply peaked at the same spatial location, they couple mainly to a small instanton (or

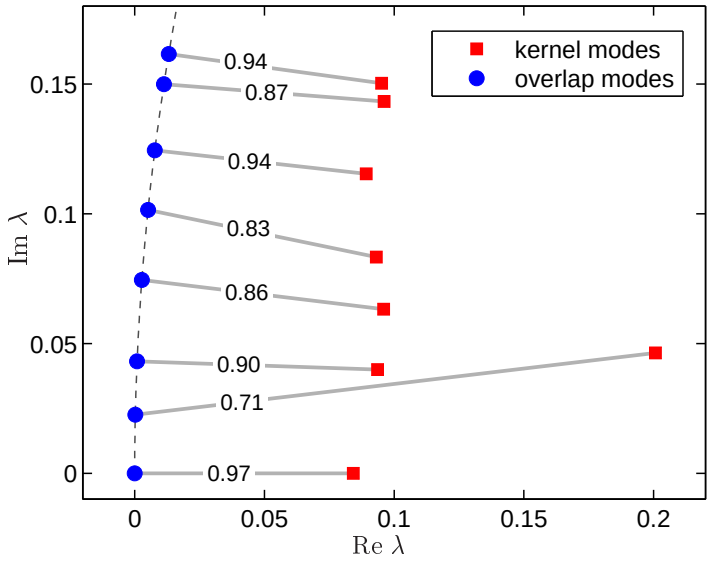

Figure 2: Eigenvalues of the kernel and overlap operator on a configuration where the overlap operator has a localized IR mode. Lines connect overlap modes with the most similar kernel modes and the magnitude of their inner product is shown.

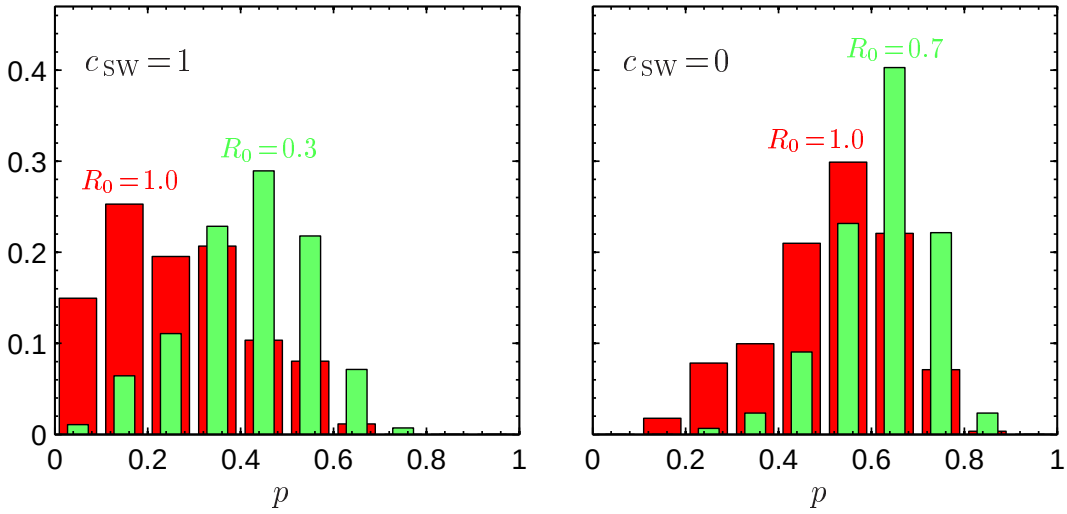

Figure 3: The distribution of the participation number of the first non-zero overlap eigenmodes in the $\nu = 1$ sector, normalized by the number of configurations.

dislocation). The overlap of the wave functions is still sizable, $\approx 70\%$, but the eigenvalues are different. The overlap eigenvalue is small, it is the most infrared among the eigenmodes. In general localized modes tend to stay localized under the overlap projection, their overlap eigenvalue is frequently small, without modifying the eigenvalues of the extended modes. Hence these non-physical eigenmodes can strongly influence the low energy structure of the systems.

To quantify the observations from Figures 1 and 2 we have measured the participation

number of the low eigenmodes of our four overlap operators. Figure 3 shows the distribution for the first *non-zero* modes in the $\nu = 1$ topological sector. The result supports what we have expected based on the eigenmodes of the kernel operator. The S1 action, that corresponds to $c_{\rm SW} = 1$ improved kernel operator with $R_0 = 1.0$, has a lot of localized modes - possibly up to 50% of the first eigenmodes are localized. The other actions are considerably better. When $R_0 = 0.3$ is used even with the clover improved action, many of the localized modes are already to the right of the overlap center and projected to the ultra-violet. Removing the clover term has a similar effect. Even with $R_0 = 1.0$, corresponding to $\Delta R_0 = 0.7$, there are only a few localized modes, and their number drops even further when $R_0 = 0.7$ ($\Delta R_0 = 0.4$) is chosen.

The localized eigenmodes are due to lattice dislocations and their number scales with the lattice volume. They are non-perturbative cut-off effects and will make the continuum extrapolation difficult. We have investigated the localization properties of the overlap eigenvalues at a finer lattice spacing but same physical volume ($\beta = 6.0$ Wilson plaquette action on 16^4 lattices) with the S2 action. The distribution of the participation numbers of the first non-zero eigenmodes was slightly worse than the corresponding distribution on the coarser lattices, making any kind of perturbative predictions difficult.

We have not investigated the localization of the overlap operator on larger physical volumes, but based on the spectrum of the kernel operator, we expect that among the first non-zero eigenmodes of the overlap operator there are as many localized modes in larger volumes as in the smaller one. These lattice artifacts are not due to finite volume effects. The localization of overlap eigenmodes have been studied recently in Refs. [7],[8], though in different context and only with a single overlap operator.

IV. CONSEQUENCES OF LOCALIZED OVERLAP EIGENMODES

In the continuum limit the eigenmodes of the Dirac operator are extended. The localized modes we observed at finite lattice spacing are lattice artifacts but their presence could influence any physical quantity that is sensitive to chiral symmetry, like the pion spectrum, the chiral condensate or the topological susceptibility. Here we study the latter two quantities.

A. The topological susceptibility

The topological susceptibility $\chi = \langle \nu^2 \rangle / V$, when defined via the index of the overlap operator, is a particularly sensitive measure of how the fermionic action observes the dislocations of the vacuum. The index of the overlap is identical to the sum of the chirality (± 1) of the real modes of the kernel operator up to $\lambda < R_0$ [9]. The real modes of the kernel operator are easiest to identify by measuring the eigenvalues of the Hermitian operator $\gamma_5 D_K$ and identifying when an eigenmodes crosses zero [10, 11]. The advantage of this approach is that one automatically obtains the topological charge for arbitrary R_0.

In Figure 4 we show the dimensionless quantity χr_0^4 as a function of R_0 for the n-HYP

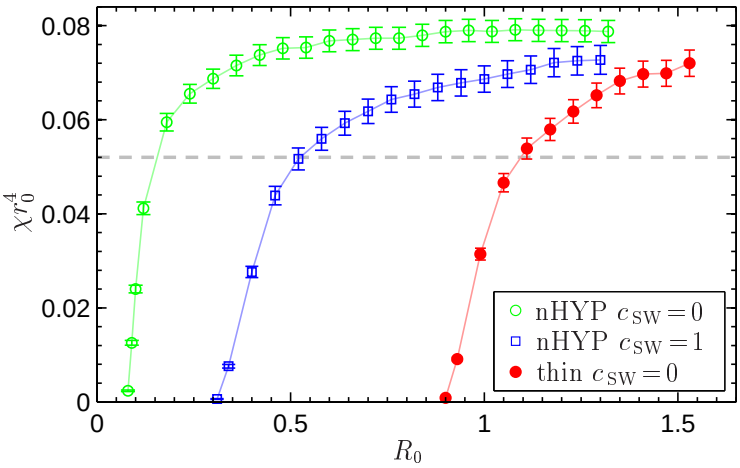

Figure 4: The topological susceptibility as a function of the overlap parameter R_0 with thin link and n-HYP smeared overlap. The dashed horizontal line is the continuum prediction from Ref. [12].

smeared $c_{\rm SW} = 0$ and 1 kernel overlap actions, and also for the unimproved thin link kernel overlap action. To set the scale we use $r_0/a = 4.032$ from Ref. [13]. We have identified the real modes of the kernel operators only below $R_0 < 1.4$ (1.6 for the thin link kernel). Had we extended these measurements further, we would have observed the susceptibility saturate, then drop again when the right edge of the first eigenvalue circle is approached, around $R_0 \approx \lambda_{\rm crit} + 2$. Recent studies of the topological susceptibility using a pure gauge $F\tilde{F}$ topological charge operator predict $\chi r_0^4 = 0.0524(13)$ [12], while calculations with a thin link overlap operator give $\chi r_0^4 = 0.059(3)$ [14] in the continuum limit. In Figure 4 we observe not only large cut-off effects, but strong dependence on the R_0 parameter, especially for the $c_{\rm SW} = 0$ actions.

The cut-off effects are the consequence of the large number of real eigenmodes toward the center of the eigenvalue circle seen in Figure 1. Most of these modes are lattice artifacts, dislocations. Overlap operators with smaller R_0 values are less sensitive to these inner modes and therefore show smaller lattice artifacts, but defining the susceptibility where the susceptibility curve is steeply rising is rather arbitrary. Since $\lambda_{\rm crit}$ depends on the lattice spacing, a small fixed R_0 value can also lead to non-monotonic or falsely flat behavior of the susceptibility as a function of the lattice spacing. Large R_0, on the other hand, creates large cut-off effects. Perhaps the most reliable continuum extrapolation with smallest lattice artifacts would come from where the parameter $\Delta R_0 = R_0 - \lambda_{\rm crit}$ is kept fixed at a small value but where the overlap operator is still local.

B. The eigenvalue distribution and the chiral condensate

The distribution of the low lying Dirac eigenmodes should follow the universal predictions of Random Matrix Theory for extended eigenmodes. Localized modes embedded in the

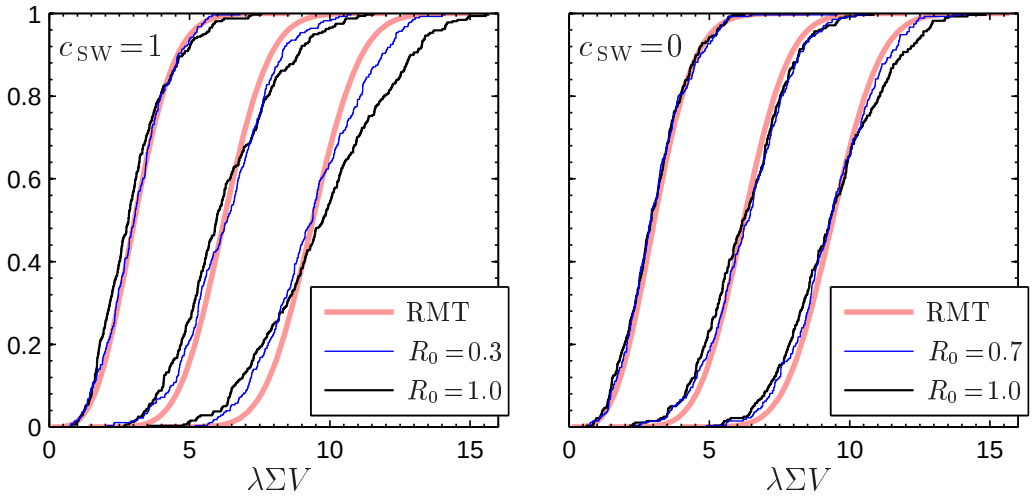

Figure 5: The cumulative distribution of the first three eigenmodes in the $\nu = 1$ topological sectors. Left panel: $c_{\rm SW} = 1$; right panel: $c_{\rm SW} = 0$. The smooth thick lines are the RMT predictions.

IR can spoil the agreement between the measured and predicted distributions. According to RMT the probability distribution of the kth eigenvalue of the Dirac operator in fixed topological sector ν is given as

$$p_{\nu,k}(\lambda) = \frac{a}{\Sigma V}\Lambda_{\nu,k} \tag{3}$$

with only one free parameter, $\Sigma V/a$, where Σ is the chiral condensate. The universal functions $\Lambda_{\nu,k}$ can be calculated analytically [1]. In numerical studies one frequently uses the cumulative or integrated distribution,

$$c_{\nu,k}(\lambda) = \int_0^\lambda dz\, p_{\nu,k}(z)\,. \tag{4}$$

Previous studies of quenched QCD found agreement with RMT predictions when averages $\langle\lambda\rangle$ or ratios of averages were considered on volumes of at least $(1.5\text{fm})^4$ for $\nu \leq 2$ and $k \leq 4$ [5], but the actual shape of the eigenvalue distributions shows significant deviations, especially for the higher modes [15, 16].

In Figure 5 we present our results for the cumulative distribution using the Dirac operators S1-S4 listed in Table I. We consider only the $\nu = 1$ topological sector, since for all 4 actions close to a third of the configurations belong there, though the other sectors give similar results. We fix the free parameter $\Sigma V/a$ by fitting the cumulative distributions to the RMT predictions. We follow the Kolmogorov-Smirnov procedure and maximize the quality factor Q ,i.e. the confidence level that the numerical data is described by the theoretical predictions [17]. The results we present here correspond to a combined fit to the lowest three modes of a given Dirac operator, but the fit results are very similar if one includes only one or two of the modes.

In Table II we give some details of the fit, including the value of $\Sigma V/a$ and the individual quality factors. Q depends exponentially on the number of configurations and on the square

action	smearing	$c_{\rm SW}$	R_0	$N_{\rm conf}$	$\Sigma V/a$	S	$S\,\Sigma V/a$	$n=1$		$n=2$		$n=3$	
								$D_{\rm max}$	Q	$D_{\rm max}$	Q	$D_{\rm max}$	Q
S1	n-HYP	0	1.0	279	90.8(2.0)	1.43	130(3)	0.056	0.335	0.081	0.047	0.090	0.021
S2	n-HYP	0	0.7	271	68.4(1.0)	1.75	120(2)	0.063	0.227	0.074	0.095	0.072	0.118
S3	n-HYP	1	1.0	318	143.2(2.4)	1.09	156(3)	0.103	0.002	0.121	0.000	0.187	0.000
S4	n-HYP	1	0.3	279	97.9(1.2)	1.36	133(2)	0.039	0.781	0.082	0.046	0.098	0.009
T1	thin	0	1.4	436	99.4(2.9)	2.80	268(8)	0.074	0.015	0.074	0.016	0.108	0.000

Table II: Results of the RMT fit of the cumulative distributions in the $\nu = 1$ topological sector. The raw data for the $T1$ action is from Ref. [5].

of the maximal deviation $D_{\rm max}$ between the predicted and measured cumulative curves. When the deviation is systematic rather then statistical, $D_{\rm max}$ is actually a better quantity to characterize the fit [18] and we list its value also in Table II. We observe significant variation in the fitted values of $\Sigma V/a$, even though the volume is the same for all actions. The renormalized chiral condensate $Z_S\Sigma$ can show cut-off effects that we cannot estimate without actually calculating the renormalization factors. However a simple calculation already shows that the Z_S factors can be very different for different overlap operators even when the same smeared kernel action is used.

To illustrate this point let us model the kernel operator as $D_K = d_{\rm ov} + \lambda_{\rm crit}$, where $d_{\rm ov}$ is an overlap operator with eigenvalues $\eta_\phi = 1 - e^{i\phi}$. Since $d_{\rm ov}$ is a normal operator, the eigenvalues λ_ϕ of $D_{\rm ov}$ in Eq. 1 can be immediately calculated. The scale factor between $d_{\rm ov}$ and $D_{\rm ov}$, $S = \lambda_\phi/\eta_\phi|_{\phi\approx 0}$ depends on the parameters R_0 and $\lambda_{\rm crit}$ and is responsible for most of the observed difference in $\Sigma V/a$. In Table II we list the values of the scale factor S and $S\,\Sigma V/a$ as well. It is interesting to note that the ratio λ_ϕ/η_ϕ can show significant dependence on ϕ when $\Delta R_0 = R_0 - \lambda_{\rm crit}$ is small even for small eigenvalues in the IR range. For us the strongest dependence is for the action S4 where the effect is $\approx 5\%$ for eigenvalues that cover the range we consider here. Once the scale factor is taken into account, the predicted values $S\,\Sigma V/a$ are consistent for the S1, S2 and S4 actions, only the S3 action with the largest deviation $D_{\rm max}$ is statistically different.

As is evident from Figure 5 and supported by the data in Table II, the first eigenmodes are well described by the RMT curve, but the agreement gets progressively worse for the higher modes. In general the $c_{\rm SW} = 1.0$ operators are worse than the unimproved ones. This is surprising as the smeared kernel action has much better chiral properties and the overlap operator is also more localized than with the unimproved kernel, however understandable if the observed lattice artifacts are caused by the localized eigenmodes.

Comparing results of the topological susceptibility (Figure 4) and the eigenvalue distributions we observe that lattice artifacts, or deviation form the continuum, correlate closely for the two observables and with the number of localized eigenmodes of the overlap operator (Figure 3). The action S2 with $c_{SW} = 0$, $R_0 = 0.7$ deviates the least from the continuum values, the action S3 with $c_{SW} = 1$, $R_0 = 1.0$ the most for both quantities.

Figure 6 compares the thin link T1 action of Ref. [5] with the S2 data [19]. These two

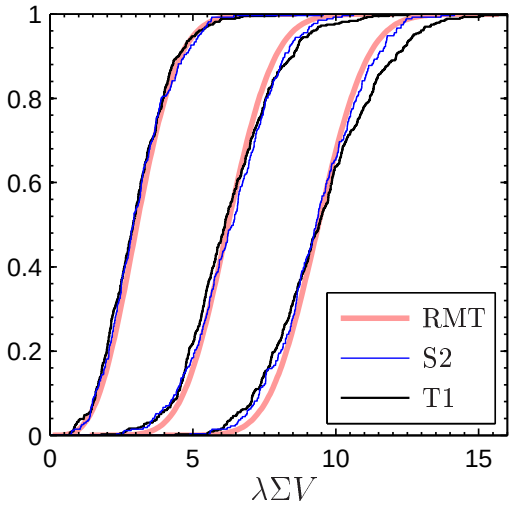

Figure 6: Same as Figure 5 but for the thin link T1 and n-HYP smeared $c_{SW} = 0$, $R_0 = 0.7$ S2 actions.

actions differ primarily in that S2 is n-HYP smeared. The smeared data agrees with the theoretical predictions better, though comparison of the T1 and S1 actions (with larger ΔR_0) shows no significant difference. Further smearing helps very little. Even with three levels of n-HYP smearing the infrared spectrum of the kernel action changes little beyond the reduction of λ_{crit}, and consequently the cumulative eigenvalue distribution of the S2 action remains very similar to the one with only one level of smearing.

The localized eigenmodes and the deviations they cause are lattice artifacts, they will disappear in the continuum limit. Nevertheless at finite lattice spacing they significantly alter the lattice results.

V. CONCLUSION AND DISCUSSION

We have investigated the localization properties of different overlap and their kernel operators in quenched systems. We found that the overlap operators can have many non-physical, localized eigenstates in the infrared. They can be related to localized modes of the kernel operator, but in the kernel operator they are typically inside the eigenvalue circle and do not directly effect the low energy spectrum. It is the overlap construction that promotes them to the infrared.

There their presence can cause significant scaling violations in quantities sensitive to the properties of the low modes. We illustrated that by comparing the eigenvalue distribution of the low energy eigenmodes to the universal predictions of random matrix theory and also by investigating the topological susceptibility. One can minimize the scaling violation effects by choosing a better kernel operator, like the n-HYP smeared operator we considered here, and by tuning the R_0 parameter of the overlap construction as small as the locality of the overlap operator would allow. Somewhat surprisingly we found that the kernel operator with the best

chiral properties, the clover improved operator, is actually worse in the overlap construction as it has the most localized modes near the IR. A chiral kernel operator reproduces itself in the overlap construction, so it is possible that other improved kernel operators behave differently. There is indication that this is indeed the case for the Fixed Point operator in Ref. [8].

In this paper we considered only quenched systems, but mixed action simulations suffer from the same problem. The localized modes of the kernel operator are far from the infrared edge and therefore are not suppressed by the fermion determinant, yet the overlap can project them into the infrared. Fully dynamical overlap simulations should fare better as there the localized eigenmodes are suppressed just like any other small eigenvalue mode, so while they are present, their number is at least not inflated. Nevertheless even in dynamical overlap simulations it is worth minimizing the occurrence of the localized eigenmodes.

VI. ACKNOWLEDGMENT

We would like to thank Profs. P. Weisz, P. Hasenfratz, P. Damgaard and T. Wettig for fruitful discussions. A.H. is grateful for the hospitality extended to her at the Max Planck Institute in Munich, and for the opportunity to use the Institute's computer cluster for part of the calculations presented in this paper. This research was partially supported by the US Dept. of Energy.

[1] P. H. Damgaard and S. M. Nishigaki, Phys. Rev. **D63**, 045012 (2001), hep-th/0006111.

[2] J. J. M. Verbaarschot and T. Wettig, Ann. Rev. Nucl. Part. Sci. **50**, 343 (2000), hep-ph/0003017.

[3] A. Hasenfratz and F. Knechtli, Phys. Rev. **D64**, 034504 (2001), hep-lat/0103029.

[4] A. Hasenfratz, R. Hoffmann, and S. Schaefer, JHEP **05**, 029 (2007), hep-lat/0702028.

[5] L. Giusti, M. Lüscher, P. Weisz, and H. Wittig, JHEP **11**, 023 (2003), hep-lat/0309189.

[6] C. Gattringer, M. Göckeler, P. E. L. Rakow, S. Schaefer, and A. Schäfer, Nucl. Phys. **B617**, 101 (2001), hep-lat/0107016.

[7] E. M. Ilgenfritz et al. (2007), arXiv:0705.0018 [hep-lat].

[8] P. Hasenfratz et al. (2007), arXiv:0707.0071 [hep-lat].

[9] F. Niedermayer, Nucl. Phys. Proc. Suppl. **73**, 105 (1999), hep-lat/9810026.

[10] R. G. Edwards, U. M. Heller, and R. Narayanan, Phys. Rev. **D59**, 094510 (1999), hep-lat/9811030.

[11] L. Del Debbio and C. Pica, JHEP **02**, 003 (2004), hep-lat/0309145.

[12] S. Durr, Z. Fodor, C. Hoelbling, and T. Kurth, JHEP **04**, 055 (2007), hep-lat/0612021.

[13] S. Necco and R. Sommer, Nucl. Phys. **B622**, 328 (2002), hep-lat/0108008.

[14] L. Del Debbio, L. Giusti, and C. Pica, Phys. Rev. Lett. **94**, 032003 (2005), hep-th/0407052.

[15] W. Bietenholz, K. Jansen, and S. Shcheredin, JHEP **07**, 033 (2003), hep-lat/0306022.

[16] W. Bietenholz and S. Shcheredin, Nucl. Phys. **B754**, 17 (2006), hep-lat/0605013.

[17] W. H. Press, S. A. Teukolsky, W. T. Vetterling, and B. P. Flannery, *Numerical recipes* (Cambridge University Press, Cambridge, 1992).

[18] A. Hasenfratz and R. Hoffmann, Phys. Rev. **D74**, 114509 (2006), hep-lat/0609067.

[19] We thank P. Weisz for sharing with us the data from Ref. [5].